Ocean Dynamics (2005) 55: 416–429
DOI 10.1007/s10236-005-0015-4

Nuno Vaz · João Miguel Dias · Paulo Leitão
Inês Martins

Horizontal patterns of water temperature and salinity in an estuarine tidal channel: Ria de Aveiro

Received: 27 January 2005 / Accepted: 26 May 2005 / Published online: 29 July 2005

Abstract This work presents results from two complementary and interconnected approaches to study water temperature and salinity patterns in an estuarine tidal channel. This channel is one of the four main branches of the Ria de Aveiro, a shallow lagoon located in the Northwest coast of the Iberian Peninsula. Longitudinal and cross-sectional fields of water temperature and salinity were determined by spatial interpolation of field measurements. A numerical model (Mohid) was used in a 2D depth-integrated mode in order to compute water temperature and salinity patterns. The main purpose of this work was to determine the horizontal patterns of water temperature and salinity in the study area, evaluating the effects of the main forcing factors. The field results were depth-integrated and compared to numerical model results. These results obtained using extreme tidal and river runoff forcing, are also presented. The field results reveal that, when the river flow is weak, the tidal intrusion is the main forcing mechanism, generating saline and thermal fronts which migrate with the neap/spring tidal cycle. When the river flow increases, the influence of the freshwater extends almost as far as the mouth of the lagoon and vertical stratification is established. Results of numerical modelling reveal that the implemented model reproduces quite well the observed horizontal patterns. The model was also used to study the hydrology of the study area under extreme forcing conditions. When the model is forced with a low river flow (1 $m^3 s^{-1}$) the results confirm that the hydrology is tidally dominated. When the model is forced with a high river flow (1,000 $m^3 s^{-1}$) the hydrology is dominated by freshwater, as would be expected in such an area.

Keywords Salinity · Temperature · Transport model · Coastal lagoon · Ria de Aveiro · Espinheiro channel

Responsible Editor: Alejandro Souza

N. Vaz (✉)
Departamento de Física, Universidade de Aveiro, Campus de Santiago, 3810-193 Aveiro, Portugal
E-mail: nuno@fis.ua.pt
Tel.: +35-1234370356
Fax: +35-1234424965

J. M. Dias
Departamento de Física, Universidade de Aveiro, Campus de Santiago, 3810-193 Aveiro, Portugal
E-mail: jdias@fis.ua.pt
Tel.: +35-1234370356
Fax: +35-1234424965

P. Leitão
Hidromod, Av. Manuel da Maia, n°36, 3°esq, 1000-201 Lisboa, Portugal
E-mail: paulo.chambel@hidromod.com

I. Martins
Departamento de Física, Universidade de Aveiro, Campus de Santiago, 3810-193 Aveiro, Portugal
E-mail: a19744@alunos.fis.ua.pt

1 Introduction

Coastal lagoons are saline water bodies separated or partially isolated from the sea. They may be enclosed by one or more barrier islands, like Ria Formosa located in Algarve (in southern Portugal), as well as sand spits and linked to the sea by one or more channels, which are small relative to the lagoon (Barnes 1977, 1980), like Ria de Aveiro (in northern Portugal).

The main driving forces of circulation in a large number of estuaries and coastal lagoons are river flow at the head of the estuary and changes in the sea level at the mouth of the estuary, which in turn determine the distribution of water properties like salinity and temperature, as well as the distribution of any other tracer. In coastal lagoons there are other forcing actions like precipitation to evaporation balance, wind stress and surface heat balance (Kjerfve 1994) and they respond differently to these forcing actions.

Ria de Aveiro is the largest coastal lagoon in Portugal and the most dynamic in terms of physical and biogeo-

chemical processes. It is a very important ecosystem in the region where it is situated due to the intense human activity in its waters and along its margins. In the last 20–30 years the lagoon was studied mainly from a biological and chemical point of view. There are not many studies or publications regarding the hydrology and physical processes of the lagoon. Despite this fact, a prior hydrologic study (Dias et al. 1999) reveals some of the main features of Ria de Aveiro. Records of water level, current velocity and thermohaline properties were performed at several stations in the lagoon during the summer seasons of 1996 and 1997. It was determined that the type of tide at the mouth of the lagoon is semidiurnal and was observed that the astronomical tide is the main forcing driving water circulation in Ria de Aveiro. The tidal wave propagation in the lagoon has the characteristics of a damped progressive wave. According to this study Ria de Aveiro was found as a vertically homogeneous coastal lagoon. Nevertheless, some channels may reveal characteristics of a partially mixed estuary, depending on the freshwater input. The importance of the freshwater sources in the lagoon dynamics and of its seasonal effects remained to study until this work. The lagoon has been also studied through numerical modelling. These studies were performed to investigate topics as the tidal propagation in the lagoon (Dias et al. 2000), the lagrangian transport of particles (Dias et al. 2001) and studies of sediment particles (Lopes et al. 2001; Dias et al. 2003).

The lagoon has several freshwater sources, Vouga River being the most important one. This freshwater source is connected to the Atlantic through a channel located in the central area of the lagoon, Espinheiro channel. The major driving force is the tide, which together with the river runoff, determines the water mass behaviour in the channel. This channel is poorly known in terms of salt and heat transport processes, even though it is ideal to perform this kind of studies in Ria de Aveiro. The description of salinity patterns provides a basis for predicting the behaviour of other soluble substances, being suitable to study since the salt is a natural tracer. This study pretends to be a first step to better comprehend the interaction between the seawater and the freshwater within this system and to the understanding of its dynamics.

These studies require an enormous amount of field data, of salinity, water temperature and current speed, as well as the implementation of numerical models that combine hydrodynamic and transport modules. This contribution uses two complementary and interconnected approaches to study the water temperature and salinity patterns in Ria de Aveiro, combining field measurements with numerical modelling results.

The main purpose of this paper is to determine the horizontal patterns of salt and water temperature in the Espinheiro channel and evaluating the importance of the main forcing mechanisms: tides and incoming river flow. To achieve this intention, a short description of the first annual observational program of the hydrological properties in Ria de Aveiro will be given. Vertical profiles of salinity and water temperature were measured along the channel. These measurements were taken at spring and neap tides and the data obtained were used to interpolate longitudinal fields of these variables. An estimation of the river flow for the survey periods was also performed. Results will be presented and discussed, that reflect the influence of river flow and spring and neap tide conditions in the spatial distribution of the referred hydrological properties. Another aim of this work is to implement a transport model in a 2D mode for the lagoon's entire area, with a closer look at its central area. The model used was Mohid—Water Modelling System, a finite volume model that combines hydrodynamic and transport modules.

2 The study area

The study area is situated in the very complex central area of Ria de Aveiro, a mesotidal and shallow (mean depth ~1 m) coastal lagoon located in the northwest Atlantic coast of the Iberian Peninsula. It includes two distinct regions: the first extending from the mouth of the lagoon to near section 5 (see Fig. 1 for reference) and the second is the Espinheiro channel, extending from section 5 to near section 10. The study area is approximately 11 km long, has an average width of about 200 m and a mean depth, along its longitudinal axis, of about 10 m. The tides are semidiurnal and they represent the major driving force of circulation in the lagoon (Dias et al. 1999).

The estimated tidal prism for the lagoon at extreme spring and extreme neap tide is 136.7×10^6 and 34.9×10^6 m^3, respectively (tidal range of about 2 m) (Dias 2001). For the Espinheiro channel is about 40×10^6 at extreme spring tide and 15×10^6 m^3 at extreme neap tide (Dias 2001). The total estimated freshwater input for the lagoon is very small (about 1.8×10^6 m^3 during a tidal cycle) (Moreira et al. 1993) when compared with the tidal prism at the mouth or at the beginning of Espinheiro channel. Despite the fact that rivers have a small contribution in terms of water input, when compared to the tidal prism, they may have a long-term influence in the residual transport (Dias et al. 2003).

Dias et al. (2000) and Dias (2001) showed that the tide is strongly distorted as it progresses from the mouth toward the end of each channel of the lagoon, due to the channels geometry and bathymetry. The general characteristics of the tidal wave are those of a damped progressive wave. In shallow areas the tidal wave assumes the main characteristics of a standing wave.

From a dynamical point of view the study area may be considered the most important in Ria de Aveiro, because here the strongest currents are observed, reaching values higher than 2 ms^{-1}. The lagoon's other

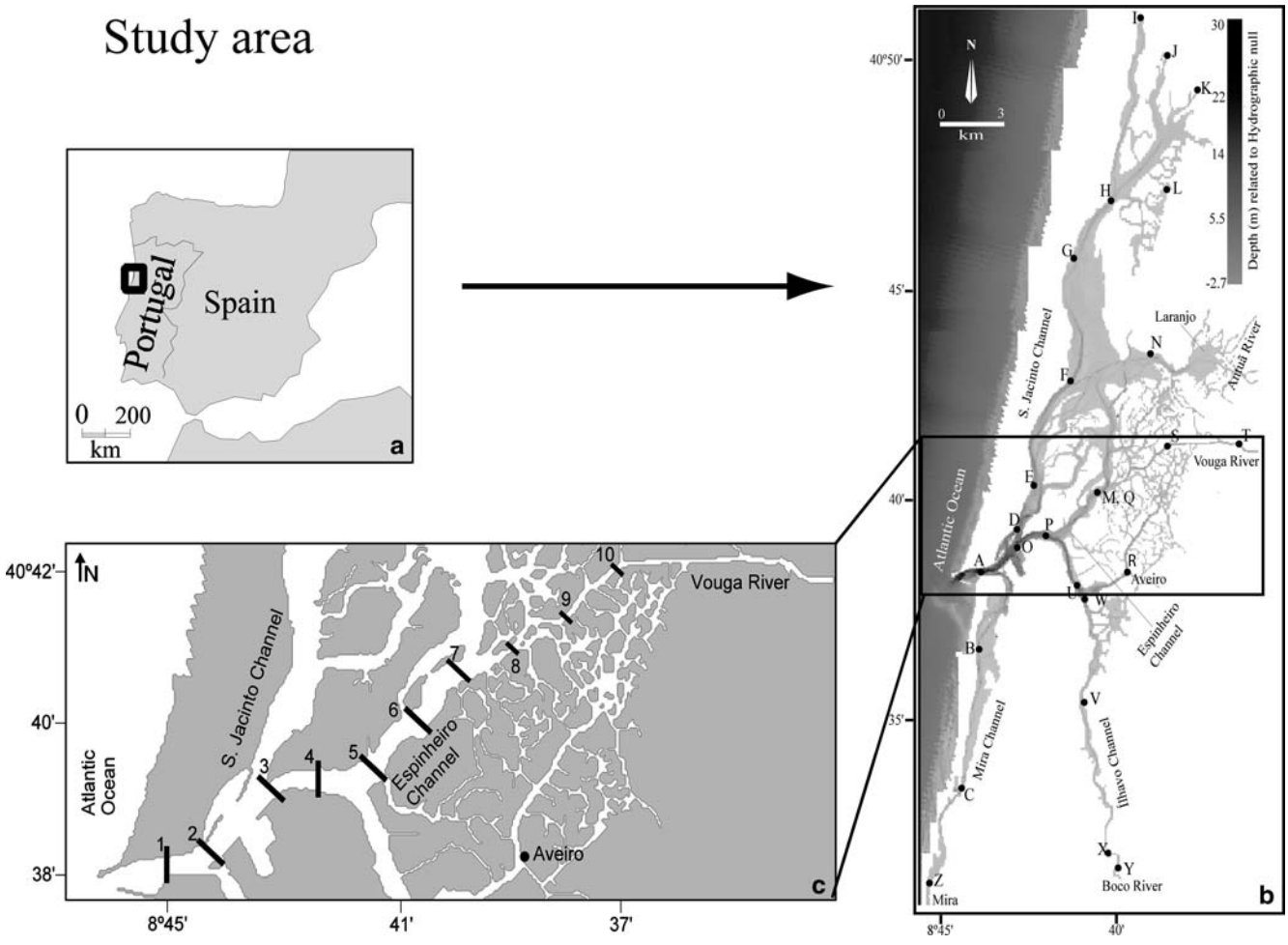

Fig. 1 Study area, with reference to the location of the stations used to calibrate the hydrodynamic and transport model and the location of the ten cross sections

channels are mainly shallow and tidal flat areas, contributing to a strong damping of currents.

3 Numerical models

3.1 The hydrodynamical and transport model

The numerical model adopted in this study was Mohid—Water Modelling System (Martins et al. 2001) developed by Maretec—Marine and Environmental Technology Center, IST, Lisbon. Mohid is a 3D finite volumes model (Chippada et al. 1998); which uses an Arakawa-C grid (Arakawa and Lamb 1977) to perform the computations. In this approach the discrete form of the governing equations are applied macroscopically to the cell control volume. The grid is therefore defined explicitly and the equations are solved using the same procedures, irrespectively of the cell geometry. Since, the equations are solved in the form of flux divergences, this method guarantees the conservation of transported properties (Ferziger and Peric 1995; Vinokur 1989). It uses an ADI—Alternate Direction Implicit scheme for the resolution of the equations. Two numerical schemes are implemented: the four equations S21 scheme (Abbot et al. 1973) and the six equations Leendertse scheme (Leendertse 1967). This model assumes the hydrostatic equilibrium, as well as the Boussinesq approximation and uses a vertical double sigma coordinate with a staggered grid.

The hydrodynamic governing equations are the momentum and the continuity equations. The hydrodynamic model solves the primitive equations in Cartesian coordinates for incompressible flows. The momentum and mass evolution equations are:

$$\frac{\partial u_i}{\partial t} + \frac{\partial (u_i u_j)}{\partial x_j} = -\frac{1}{\rho_0}\frac{\partial p_{\text{atm}}}{\partial x_i} - g\frac{\rho(\eta)}{\rho_0}\frac{\partial \eta}{\partial x_i} - \frac{g}{\rho_0}\int_{x_3}^{\eta}\frac{\partial p'}{\partial x_i}\mathrm{d}x_3 + \frac{\partial}{\partial x_j}\left(\upsilon\frac{\partial u_i}{\partial x_j}\right) - 2\varepsilon_{ijk}\Omega_j u_k \quad (1)$$

$$\frac{\partial \eta}{\partial t} = -\frac{\partial}{\partial x_1}\int_{-h}^{\eta} u_1 \mathrm{d}x_3 - \frac{\partial}{\partial x_2}\int_{-h}^{\eta} u_2 \mathrm{d}x_3 \quad (2)$$

where u_i are the velocity vector components in the Cartesian x_i directions, η is the free surface elevation, ν is the turbulent viscosity and p_{atm} is the atmospheric pressure. ρ is the density and ρ' its anomaly, ρ_0 is the reference density, g is the acceleration of gravity, t is the time, h is the depth, Ω is the Earth's velocity of rotation and ϵ is the alternate tensor.

The model also solves a transport equation for salinity and temperature or any tracer. The advection–diffusion equation reads:

$$\frac{\partial \alpha}{\partial t} + u_j \frac{\partial \alpha}{\partial x_j} = \frac{\partial}{\partial x_j}\left(K \frac{\partial \alpha}{\partial x_j}\right) + FP \tag{3}$$

where α is the transported property, K is the diffusion coefficient and FP is a possible source or sink term.

The bottom shear stress τ is imposed using the formulation proposed by Chézy (Dronkers 1964), whereτ is proportional to the velocity squared (Eq. 4) and the drag coefficient (C_D) can be parameterised in terms of the Manning friction coefficient (n) (Eq. 5):

$$\tau = C_{\mathrm{D}} |\mathbf{V}| \mathbf{V} \tag{4}$$

$$C_{\mathrm{D}} = g n^2 H^{-1/3} \tag{5}$$

where $\mathbf{V}$ is the horizontal velocity vector, n is the Manning coefficient and H is the depth of the water column.

3.2 Boundary conditions

Five types of boundaries were used in this study: free surface, bottom, lateral closed boundary, lateral opened boundary and moving boundary.

Elevation at the open boundary is specified from the tidal constituents obtained using measurements of sea surface elevation from a tidal gauge located at the mouth of the lagoon. Salinity and water temperature are also imposed at the ocean open boundary and are considered constant in this work. At the river boundaries the river flow is imposed and salinity and water temperature are assumed constant in each simulation (varying in each case study). The lateral boundary condition at coastal boundaries is a free slip condition, imposed by specifying a zero normal component of mass and null momentum diffusive fluxes at cell faces in contact with land. No fluxes at the bottom and surface were considered. Moving boundaries are closed boundaries whose position varies in time. This situation occurs in domains with intertidal zones like Ria de Aveiro. In this case the uncovered cell must be tracked. A criterion based on Fig. 2 is used.

HMIN is a minimum depth below which the cell is deemed to be dry, thus, conserving a thin volume of water above the uncovered cell. The cells in position i, j are considered uncovered when one of the two following conditions occurs:

$$H_{ij} < \mathrm{HMIN} \quad \text{and } \eta_{\mathrm{ij}-1} < -h_{ij} + \mathrm{HMIN} \tag{6}$$

$$H_{ij-1} < \mathrm{HMIN} \quad \text{and } \eta_{\mathrm{ij}} < -h_{ij-1} + \mathrm{HMIN} \tag{7}$$

where $H = h + \eta$ is the total depth. The second condition of Eq. 6 assures that the cell is not being covered by waves propagating from left to right and the second condition of Eq. 7 assures that the cell is not being covered by waves propagating from right to left. The model performs the same test in the i direction. The noise resulted from the abrupt variation in the velocity of the dry cells is controlled by a careful choice of HMIN (in this case HMIN = 0.1 m) (Leendertse and Liu 1978).

3.3 Application to the Ria de Aveiro

Due to the lagoon complex geometry and in order to decrease the computational effort a variable spatial grid step was developed. This grid has 429 × 568 cells, with dimensions ranging from 40 × 40 m^2 (to obtain a higher resolution) in the central area of the lagoon where the channels are very narrow (represented in Fig. 1c), to 40 × 100 m in the northern and southern areas, due to the orientation of the channels (north–south). The numerical bathymetry used was developed from data concerning depth obtained from a general survey carried out by the Hydrographic Institute of the Portuguese Navy in 1987–88. More recent bathymetric data, obtained from recent dredging operations in several channels (1998) and close to the lagoon's mouth (2002), were also used. The water depth at each grid point was computed, from the water volume of the cell, using a Monte Carlo cubature method (Dias 2001).

The model was forced imposing at the oceanic open boundary the sea surface elevation determined from 38 tidal constituents, obtained through harmonic analysis (Pawlowicz et al. 2002) of values, measured during 2002 in a tidal gauge located at the mouth of the lagoon. At this open boundary the water temperature and salinity were considered fixed in each simulation, with values of 15°C and 36 practical salinity units (psu), respectively. At the channel's head river flow values estimated for the survey periods, with values between 2 m^3 s^{-1} and 116 m^3 s^{-1} were imposed. The water temperature and salinity of Vouga River were fixed for each simulation, with values ranging between 22°C (September) and 11°C (December) for the water temperature and a fixed value of 1 psu for the salinity. The time step is 10 s and the horizontal viscosity is 5 m^2 s^{-1}. Initial conditions for the hydrodynamic model are null free surface elevation and null velocity in all grid points. For the transport model these are salinity and water temperature fields, obtained by interpolation of data collected in the study area on the autumn of 2003. For the transport model more realistic initial values were adopted because the time to reach dynamic equilibrium for these variables is much longer than that for tides and tidal currents. A value of

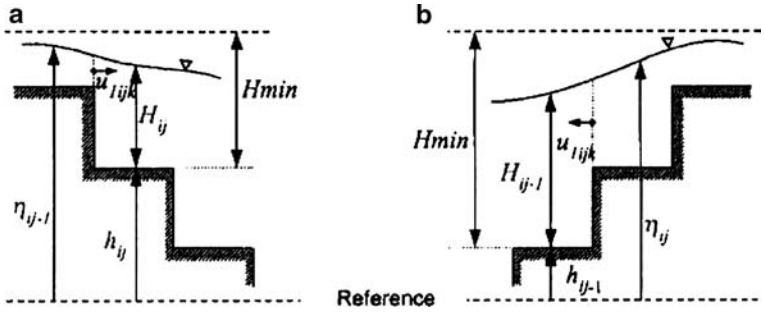

Fig. 2 Conditions for a point to be considered uncovered

5 m^2 s^{-1} was adopted for both salt and heat diffusion coefficients.

The numerical model was implemented in a 2D horizontal mode for the entire area of the lagoon. The goal was to reproduce the distribution patterns of salinity and water temperature in the entire lagoon, with a closer look at the study area described in section 2. Several simulations were performed in order to reproduce various field survey periods and to determine the horizontal patterns of salinity and water temperature under extreme tidal and river flow forcing conditions.

The hydrodynamic model was previously calibrated (Vaz et al. 2004) and validated for Ria de Aveiro. From the observation of sea surface elevation data it is concluded that there is tidal energy damping, due to friction, as the tidal wave propagated toward the end of the channels. In the case of Ria de Aveiro this behaviour was analysed by Dias and Fernandes (2005). The magnitude of the bottom friction coefficient determines changes in the tidal wave propagation within the lagoon. The bottom roughness was parameterised from Manning coefficients; therefore the model parameter subjected to adjustments in the calibration process is the Manning bottom friction coefficient. The procedure used to calibrate the model consisted in spatially varying the bottom roughness by assigning Manning values to specific regions of the numerical domain.

The calibration procedure was performed by comparing the harmonic constituents of the main tidal constituents determined from computed time series of sea surface elevation to those obtained from observed data for 24 stations located throughout the main channels of the lagoon. The data available were 1987 and 1988 data obtained from a field survey carried out by the Portuguese Navy. The better adjustment between computed and observed data were obtained for Manning coefficients ranging between 0.022 $m^{1/3}$ s^{-1} and 0.045 $m^{1/3}$ s^{-1}. Figure 3 shows the comparison for the M_2 constituent, which is the most important tidal constituent in this lagoon. It represents over 90% of the tidal energy in Ria de Aveiro. For this constituent the mean phase and amplitude difference, for all 24 stations, is 3° and 3 cm, respectively. One error of 1° corresponds to about 2 min departure in the arrival of high tide for a

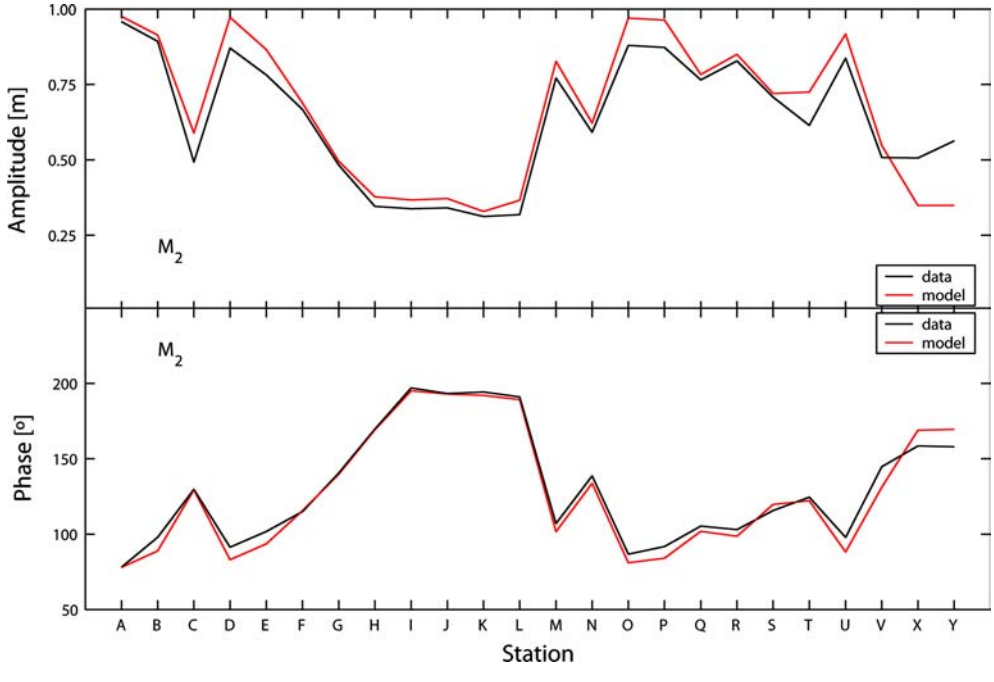

Fig. 3 Comparison between tidal amplitude and phase for M_2 constituent for data and model results, plotted on each station used in the model calibration

semidiurnal constituent, which means that the average difference between field and model data is about 6 min for the M_2. The validation procedure consisted in comparing simulated sea level and current velocities with observed data for 11 stations obtained in the summer of 1997. The root-mean squared errors (RMS) of the sea level values are typically around 5% of the local tidal amplitude. A current velocities comparison for three stations is presented in Fig. 4. Regarding current velocity there are some discrepancies between the field and model data when assessing point by point. The RMS error for these three stations is lower than 30% of the current amplitude (the better adjustment is for station D with a RMS error of 6%). Nevertheless, the model does properly simulate the temporal variation of the current velocity considered in terms of the current phase.

Results of the calibration and validation processes indicate that a good implementation of the hydrodynamic model was achieved. The agreement between computed and observed time series of sea surface elevation rounds a RMS of 5% of the local tidal amplitude for almost all the stations. Also, a good agreement for current velocities was achieved as shown in Fig. 4. When comparing current velocities values it is important to remember that this variable varies rapidly in space, both in magnitude and direction, from point to point. This behaviour reflects the irregular area geometry and it produces higher discrepancies between field and model results. Besides, the model results are related to the mean value over the vertical and horizontal spatial domain corresponding to the grid size, while the field data corresponds to a single point or, at best, an average over various points.

The transport model was also calibrated. This procedure was achieved by comparing computed and observed short-time series of salinity and water temperature for seven stations in the lagoon. The available data were from July 1996, representing a typical summer situation. A salinity and water temperature comparison for station B is depicted in Fig. 5, showing a good agreement between computed and observed data of salinity and water temperature. During the low tide were found differences of about 1 and 3 psu between the model and field salinity data for all the stations used in the transport calibration. At the high tide, the differences are lower than 1 psu. Regarding the water temperature, were found differences, at low tide, of about 3°C in some of the stations. In shallow systems like Ria de Aveiro the water temperature is ruled not only by the tidal propagation and the incoming river flow but also by meteorological factors. The air temperature, relative humidity, cloud cover and incoming solar radiation are very important due to the small depth of the water column. In the future, to improve the water temperature results, the exchanges between the water and the air will be included in the runs. Despite this fact, after these results both the hydrodynamical and transport models can be considered calibrated.

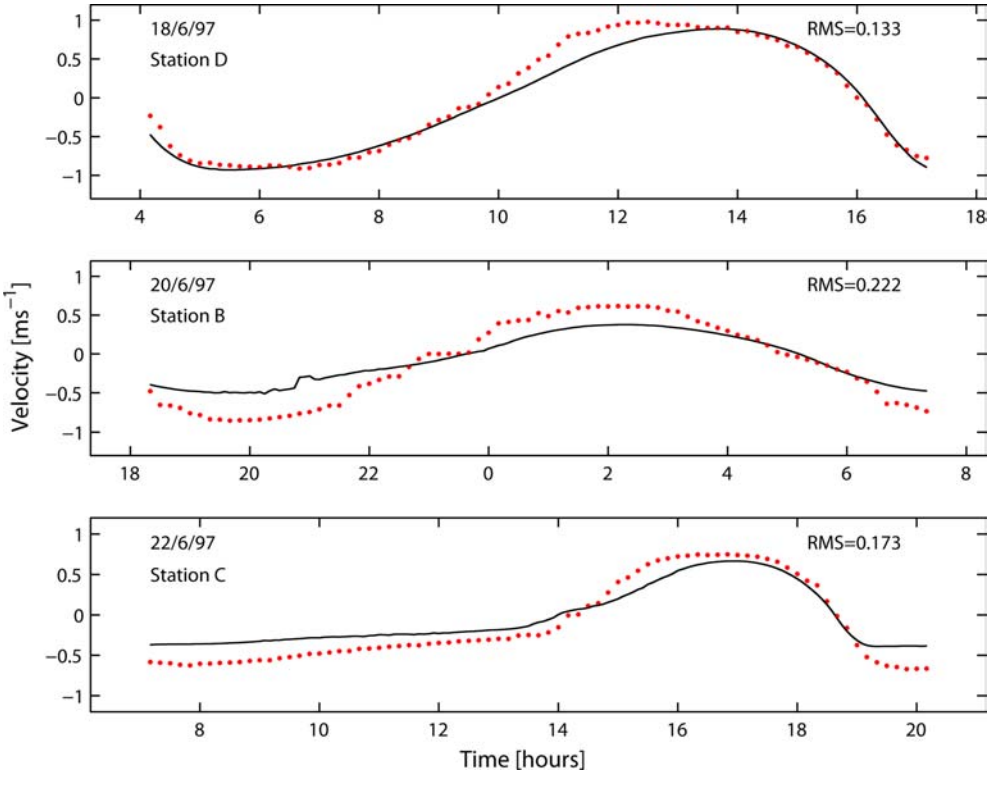

Fig. 4 Comparison between time series of main flow directions velocities of data (*dots*) and model results (*line*), plotted for some of the stations used in the model validation

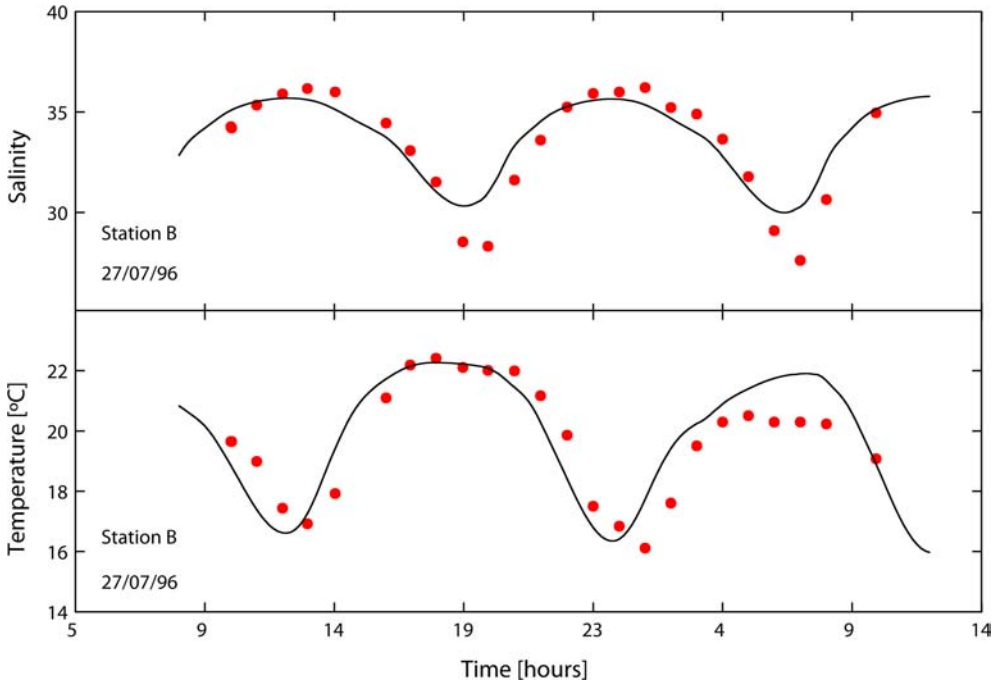

Fig. 5 Comparison between data (*dots*) and model results (*line*) time series of salinity and water temperature, for one station used in the calibration of the transport model

4 Field surveys

4.1 Materials and methods

In situ vertical profiles of hydrological properties, such as water temperature and salinity were measured in ten cross-sections (Fig. 1) separated by 1,000 metres us ing a mini STD model SD204. The survey period lasts from September 2003 until September 2004, but for the purpose of this study only the autumn results are analysed (see Table 1).

The first cross-section is located near the mouth of the lagoon and the last one is located near the channel's head, close to the mouth of the Vouga River. The in situ measurements were performed two times per month at spring tides (maximum of tidal amplitude) and at the following neap tide (minimum of tidal amplitude) and started approximately 1 h 40 min after the low-tide hour predicted for section 1, during the flood stream. The profiles of salinity and water temperature were obtained at three points in every section: near the margins of the channel and in its axis.

Table 1 Autumn sample periods

Date	Tide	Tidal height [m]	River flow [m^3 s^{-1}]
26/09/2003	Spring	2.8	2.06
02/10/2003	Neap	1.6	6.11
28/10/2003	Spring	2.8	5.44
06/11/2003	Neap	2.0	52.62
25/11/2003	Spring	2.8	72.74
05/12/2003	Neap	1.7	115.97

In order to obtain the incoming freshwater flow from Vouga River, concurrent with the survey periods, measurements of current speed were also performed. These measurements were obtained using a Valeport current meter model 105 and were performed several kilometres upstream from the river mouth, 3 h after the low-tide hour predicted for the lagoon's mouth. This procedure guarantees that the measurements of current speed were made outside the region of tidal flood influence.

Longitudinal and cross-sectional fields of water temperature and salinity were determined by spatial interpolation of the measured data using an ordinary Point–Krigging method (Cressie 1993). The longitudinal fields were computed for three different depths: near surface, half water column and near the channel's bed. Depth integrated longitudinal fields of water temperature and salinity were also computed. These last results were compared to the results of the 2D depth-integrated model used in this study. These longitudinal fields act like synoptic snapshots of the channel in terms of water temperature and salinity.

5 Results and discussion

After being calibrated the hydrodynamic and transport models have been used to study the hydrodynamics and transport of salt and heat in Ria de Aveiro. Several runs were performed to characterise the dynamics of the lagoon, with a closer look at its central area, in terms of the water temperature and salinity behaviour, considering different tidal and river runoff forcings.

Short runs of the model were carried out, covering the field survey periods for several spring/neap cycles in

the autumn of 2003. The results of the model simulations were compared to the field results to prove the ability of the implemented model to reproduce the salinity and water temperature patterns in the study area.

In order to analyse the behaviour of the study area under extreme conditions several runs of the model were also performed under conditions of high/low river runoff and astronomical tide forcing (neap/spring tidal forcing).

For the entire study area and for extreme conditions of river runoff and tidal forcing the fractional freshwater concentration (Dyer 1997) was also computed:

$$f = 1 - \frac{S_n}{S_s} \tag{8}$$

where S_s is the salinity of the undiluted sea water and S_n is the mean salinity in a given segment of the estuary. The goal was to determine the relative importance of spring or neap tide forcing and of high or low river runoff forcing in the establishment of salinity and water temperature patterns in the study area.

5.1 Field surveys

The mean Vouga River runoff estimated for the period from September to December was about 42.5 $m^3 s^{-1}$, with a minimum value of 2.06 $m^3 s^{-1}$ (September) and a maximum of 115.97 $m^3 s^{-1}$ (December). The autumn of 2003 may be considered a dry season when compared to previous years (Dias 2001). Results of salinity and water temperature for these extreme cases will be analysed and discussed. In this period the tidal amplitude ranges from a minimum of 1.6 m on October 2nd and a maximum of 2.8 m in all the spring's dates.

Figure 6 illustrates the differences in the distribution patterns of salinity in the case of two neap-tide periods (tidal amplitudes of 1.6 and 1.7 m) and in conditions of low and high river flow (6.11 and 115.97 $m^3 s^{-1}$) for three different depths: surface, mid-water and near the bed. In the case of the low river flow, the channel can be considered nearly vertically homogeneous and highly saline, almost as far as section 8, where a saline front is observed. Close to the channel's head, the relative effect of the freshwater inflow increases and values of salinity between 6 (surface) and 11 psu (bottom) are observed. For the high river flow, the effect of the freshwater extends to the mouth of the lagoon, mainly in the surface layer, leading to vertical stratification (near the surface, the salinity is about 22.5 psu and near the bottom is about 32.5 psu).

The longitudinal gradients of water temperature are less perceptible (weaker) than those of salinity, both in spring and neap tide conditions. As an example, the

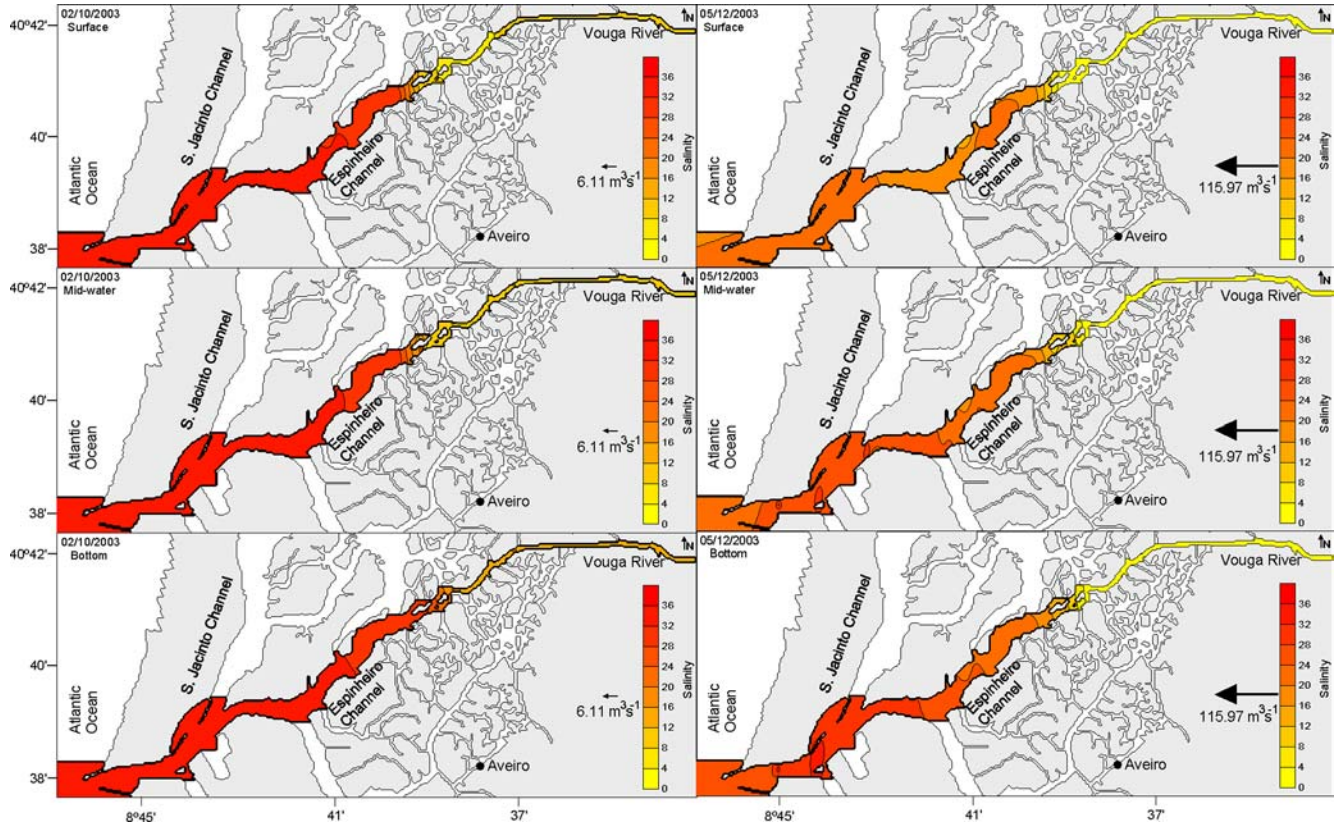

Fig. 6 Surface, mid-water and bottom salinity distributions. Neap-tide periods of 2/10/2003 and 5/12/2003. River flow of 6.11 $m^3 s^{-1}$ and 115.97 $m^3 s^{-1}$

water temperature values ranges between 11 and 14°C in the neap-tide period of December 5th, while the salinity gradient ranges between 0 and 28 psu (depth average values). However, the temperature patterns are similar to those discussed for the salinity.

The effect of the river runoff increase at the mouth of the lagoon is shown in the cross-sectional distribution of salinity at section 1 for the cases presented in Fig. 6. These results (see Fig. 7) reveal the influence of the low and high river flow at section 1. When the river flow is weak, the cross-sectional distribution of salinity is almost vertically homogeneous and the water column is mostly saline. When the river runoff is high, the freshwater influence is felt even at the lagoon's mouth, being established a vertical gradient of salinity, ranging from ~20 at the surface to ~35 psu at the bottom. At the channel's head the river flow induces an opposite effect. When the river flow is high the cross-sectional salinity distribution is almost vertically homogeneous (water column characterized by freshwater) and when the river flow is weak a vertical stratification is established.

The field results show that when the river flow is weak (with values ranging between 2 and 6 $m^3 s^{-1}$), the saline intrusion goes further along the channel than under strong freshwater runoff. Even in the case of low river flow, the channel's head is mainly filled by freshwater and as the saline intrusion goes further along the channel's bed than along the surface, the vertical stratification is higher near the channel's head than in the rest of the channel. In these cases the hydrodynamics of the

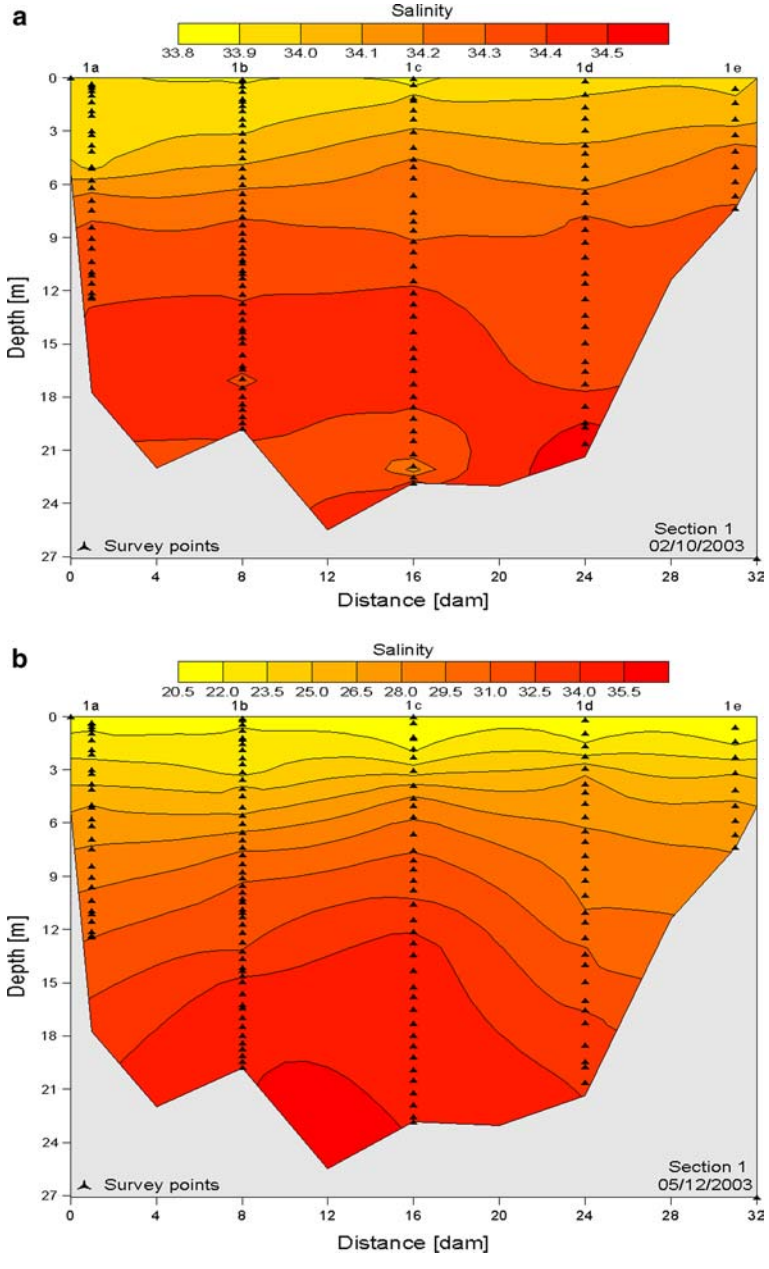

Fig. 7 Salinity cross sections at section 1. Survey days: neap-tide periods of **a** 2/10/2003 and **b** 5/12/2003. River flow of: **a** 6.11 $m^3 s^{-1}$ and **b** 115.97 $m^3 s^{-1}$

study area are determined mainly by the tide. In the opposite case, when the river flow is high, the freshwater extends its influence toward the lagoon's mouth leading to vertical stratification along most of the channel.

Saline and thermal fronts are generated between sections 8 and 9 in spring tide periods. These fronts are probably generated as a response to bathymetric features and river runoff variability. In this region, the channel's depth changes abruptly (from 10 m to ~2 m) and the tidal excursion reaches the region of freshwater influence, where the salty water (more dense) mixes with the incoming freshwater leading to a pronounced horizontal gradient of salinity and water temperature. These fronts could migrate with the spring/neap tidal cycle and with changes in the river flow. In fact, these fronts are the boundary between two distinct areas of this channel: the first one extends from the mouth of the lagoon until near section 7 and it is dominated by the tidal flux; the other is one area that could be considered as the fluvial estuary of the Vouga River, being characterised by freshwater inputs but still subjected to tidal effects.

At neap tides, these strong horizontal gradients are observed between sections 7 and 8, about 1 km closer to the mouth of the lagoon, because the saline intrusion does not extend so far in this case due to smaller tidal prisms and current velocities.

For similar freshwater inputs the salinity difference between the mouth of the lagoon and the channel's head is larger at neaps than at springs, when the tidal currents are stronger and the oceanic water intrusion goes further within the channel. The relative effect of the river flow in the horizontal patterns of salinity and water temperature is stronger at neaps, when the tidal currents are weaker.

In Fig. 8 are depicted the along channel depth averaged salinity (8a and 8b) and water temperature (8c and 8d) values. From 8a and 8b is perceptible that when the river flow is similar (September and October data) the tidal excursion goes further upstream in spring than in neap tide (~1 km), due to the higher velocity currents. When the end of the autumn is closer, the river flow increased and its effect became more important in the establishment of the salinity patterns than the tidal effect. The freshwater influence extends itself until section 6. When the river flow is 115.97 $m^3 s^{-1}$, the influence of the freshwater extends almost section 3 (1 km from the mouth of the lagoon) with salinities lower than 30 psu.

Figures 8c and 8d show the autumn variation of the water temperature along the channel. It can be observed that the water temperature values decay along the season and that exists an inversion of the temperature gradients between the beginning of the autumn and its end. In fact, in September and October the oceanic temperatures values are lower than the river ones, and in November and December it is noticeable the opposite. The figures previously depicted show that the sample strategy is correct and the data are reliable.

5.2 Observed data/model data

Model simulations were performed for the periods corresponding to the field surveys, forcing the model with the freshwater inputs determined in the field work. The purpose of these short simulations was to find out if the numerical model is able to reproduce the measured saline and thermal fronts in such a complex area.

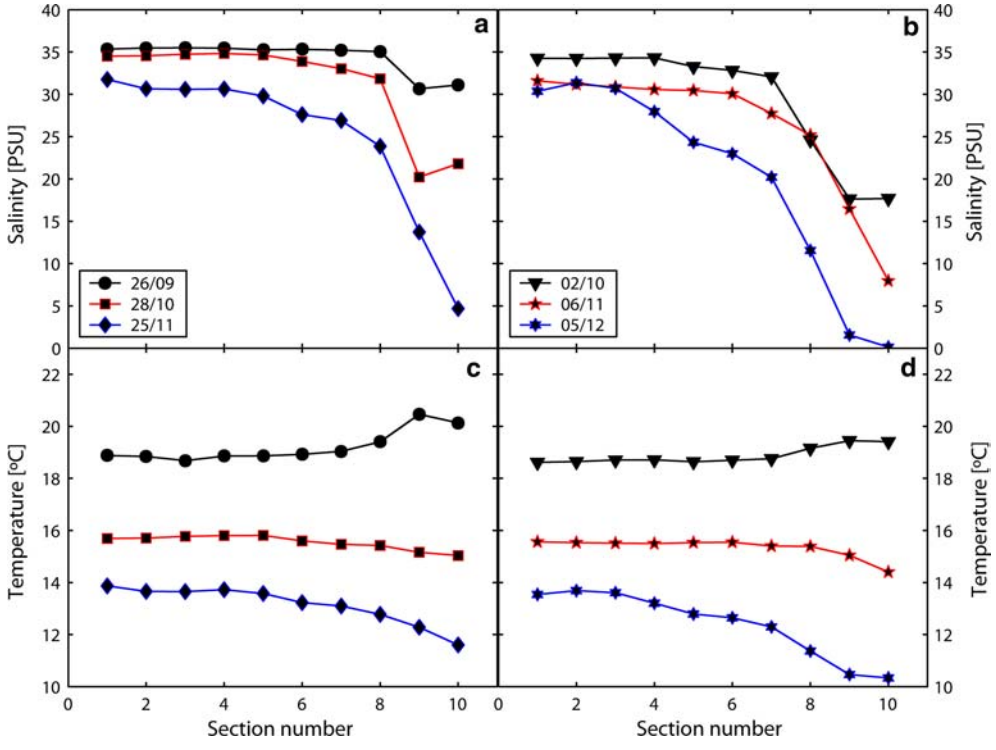

Fig. 8 Depth-averaged along channel salinity and water temperature values. Springs (8a and 8c): 26/09 (river flow = 2.06 $m^3 s^{-1}$), 28/10 (river flow = 5.44 $m^3 s^{-1}$) and 25/11 (river flow = 72.74 $m^3 s^{-1}$). Neaps (8b and 8d): 02/10 (river flow = 6.11 $m^3 s^{-1}$), 06/11 (river flow = 52.62 $m^3 s^{-1}$) and 05/12 (river flow = 115.97 $m^3 s^{-1}$)

Figure 9 shows the numerically computed and observed depth integrated fields of water temperature for the neap-tide period of October 2nd (low river flow–6.11 $m^3 s^{-1}$) and December 5th (high river flow–115.97 $m^3 s^{-1}$). The results of the 2D depth integrated model are consistent with the measurements, as shown in the figure. The model results and the measurements reveal similar patterns in the longitudinal distribution of salinity (not shown) and water temperature. The thermal and saline (not shown) fronts are well reproduced by the model as shown in Fig. 9a and 9b. The model results show the thermal front placed in exactly the same area as revealed by the measurements. When the river flow increases, the effect of the freshwater inflow in the channel is well reproduced by the transport model. The numerical results reproduce the observed longitudinal gradient of water temperature, which extends from the channel's head until the lagoon's mouth, where values of 14°C are observed in both situations. Therefore, it can be considered that a 2D depth integrated model is a reliable tool to study transport processes in shallow areas like Ria de Aveiro.

5.3 Salinity and water temperature distributions under extreme forcing conditions

Once the numerical model is considered able to reproduce the reality it can be used to perform several other studies. One of these studies is to evaluate how the study area responds to changes in the forcing factors and determine the establishment of salinity and water temperature longitudinal patterns under different conditions. As previously proved these studies can be performed using the model in a horizontal 2D mode. In this case the simulations were performed under extreme forcing conditions of astronomical tidal forcing and high and low river flow.

Vicente (1985) presents values correspondent to flood flows for periods of 25 and 100 years of 3,400 and 4,100 $m^3 s^{-1}$, respectively. Other studies (Castanho 1968) present values for the maximum daily flow, for return periods of 1, 5, 10 and 25 years, of 505, 875, 960 and 1,020 $m^3 s^{-1}$. Meanwhile, Castanho (1968), present values of minimum flow of the order of 1 $m^3 s^{-1}$. The model simulations were performed using river flows of 1 $m^3 s^{-1}$ and 1,000 $m^3 s^{-1}$. These values can be considered extreme taking into account the values presented in this paragraph.

Figure 10 shows results of the longitudinal salinity fields for 2 different situations: (a) spring tide combined with river flow of 1,000 $m^3 s^{-1}$ during high tide and (b) neap tide with river flow of 1,000 $m^3 s^{-1}$ during low tide. The 2D depth integrated results using a river flow of 1 $m^3 s^{-1}$ are not shown because they are almost redundant concerning the results shown in section 5.1.

When the low tide is reached, the model results are in agreement with the expected pattern of salinity both in spring (not shown) and neap-tide periods. In fact, these results reveal that, in this case, the freshwater extends throughout all the study area (including the coastal zone) revealing that the Vouga River influence is very important in the establishment of the hydrology of the study area during flood periods. Therefore, due to the relatively small channel dimensions very low salinity values are obtained for the outside of the lagoon both in neap-tide period (between 7 and 9 psu) and in spring tide period (between 5 to 8 psu) when the currents are higher.

During flood periods, the tide pushes the freshwater upstream revealing that, even in this extreme situation of river flow, the salinity intrusion is very significant along the length of the study area. When the high tide is

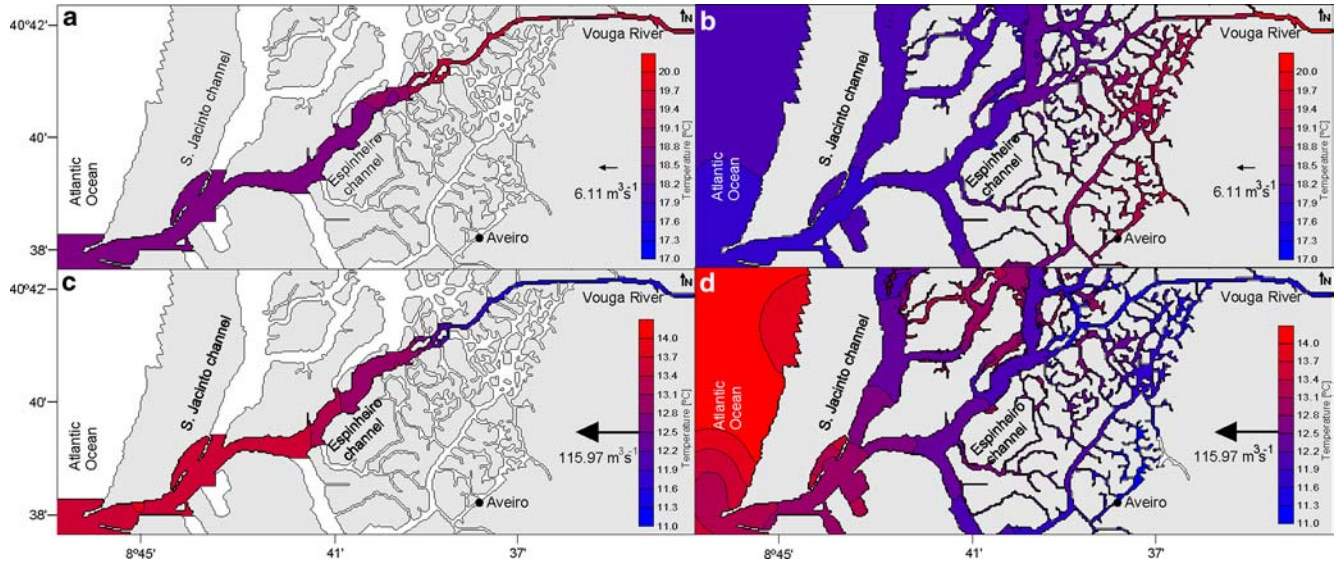

Fig. 9 Depth-integrated water temperature fields. **a** and **c** field data, **b** and **d** computed data. **a** and **b** neap-tide period of 02/10/2003, river flow of 6.11 $m^3 s^{-1}$ and **c** and **d** neap-tide period of 05/12/2003, river flow of 115.97 $m^3 s^{-1}$

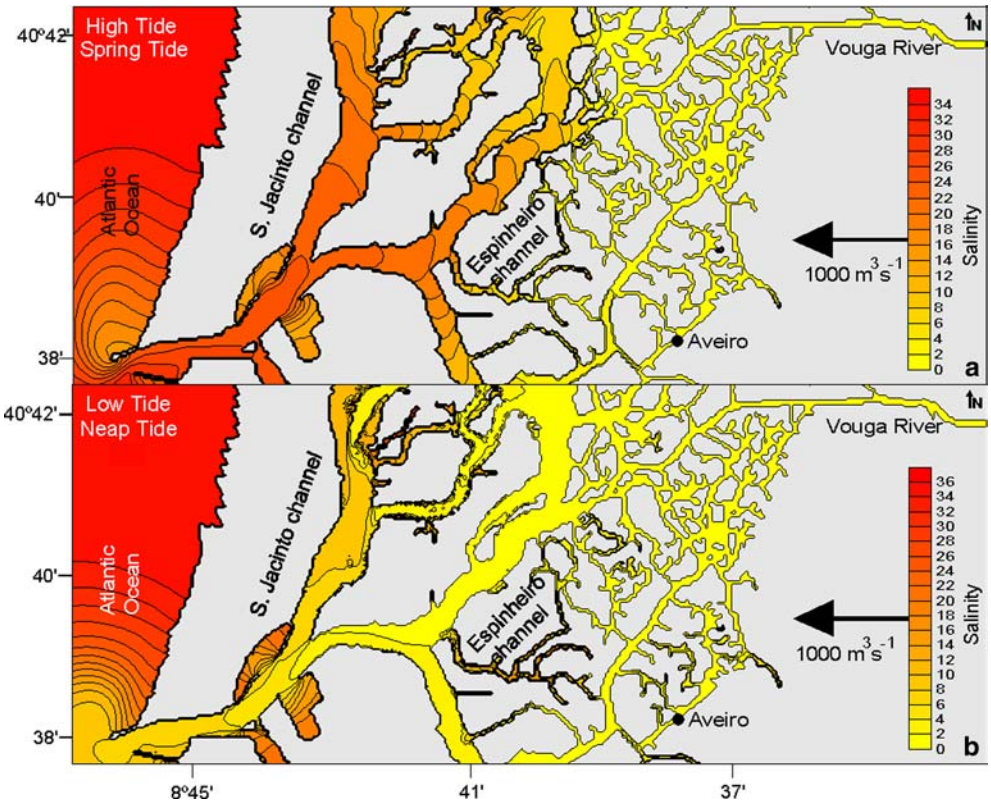

Fig. 10 Depth integrated salinity fields (model results). **a** High tide, spring tide, river flow of 1000 $m^3 s^{-1}$. **b** Low tide, neap tide, river flow of 1000 $m^3 s^{-1}$

reached, a longitudinal salinity gradient is established both at neaps (not shown) and springs. However, even at high tide, salinity at the lagoon's entrance is lower than the typical ocean values (around 36 psu), as found in the previous cases of low river flow. The freshwater that leaves the lagoon during the ebb dilutes the oceanic water in the coastal region near the lagoon's mouth. During the flood this freshwater enters the lagoon and mixes with the freshwater incoming from Vouga. The values of salinity in the mouth of the lagoon are between 22 and 25 psu in spring and neap tide, respectively. The patterns of water temperature are the same as the discussed for salinity.

The fractional freshwater concentration (Dyer 1997) was also computed for two of the studied situations: minimum freshwater and maximum freshwater within the estuary. The results are depicted in Fig. 11 and show that the minimum amount of water within the channel occurred in spring tide conditions with a low river flow of 1 $m^3 s^{-1}$ when the high tide is reached (Fig. 11a). In this case, values lower than 0.1 were found almost up to the channel's head, revealing that in the study area, there is almost no dilution of the salt water coming from the ocean. The saline intrusion goes further upstream than in any other case and the channels are filled with salt water. In this situation the hydrology is completely tidally dominated. The maximum freshwater within the channel occurred in the case of neap tide conjugated with an extreme river flow of 1000 $m^3 s^{-1}$, when the low tide is reached (Fig. 11b). Values ranging between 0.7 and 0.8 were found from the channel's head up to the lagoon's mouth. In this case the hydrology of the channels is strongly dependent on the Vouga River forcing and the study area is filled with freshwater.

6 Conclusions

The spatial and temporal distribution of hydrological properties, like salinity and water temperature, in a system like the one studied in this work, is strongly dependent on the balance between the spring/neap tidal cycle and the river flow. Observations reveal the existence of vertical stratification in the study area when the river runoff is high. The salty water, more dense, develops within the channel through the bottom layer, near the channel's bed, and the freshwater through the top layer, revealing a typical estuarine behaviour.

Results obtained using field data show a strong horizontal gradient of salinity and water temperature which migrates with the spring/neap cycle. This strong horizontal gradient seems to mark the boundary between two distinguished sectors: a marine estuary, in close connection with the sea and an upper fluvial estuary characterised by the freshwater from the river but still subject to a semidiurnal tidal effect. In this channel, for low river flow, these estuarine fronts migrate from between section 7 and 8 to between section 8 and 9 (about 1 km), depending if the tide is a neap or a spring one, respectively.

The model used in a 2D horizontal depth integrated mode reproduces the main features found from the

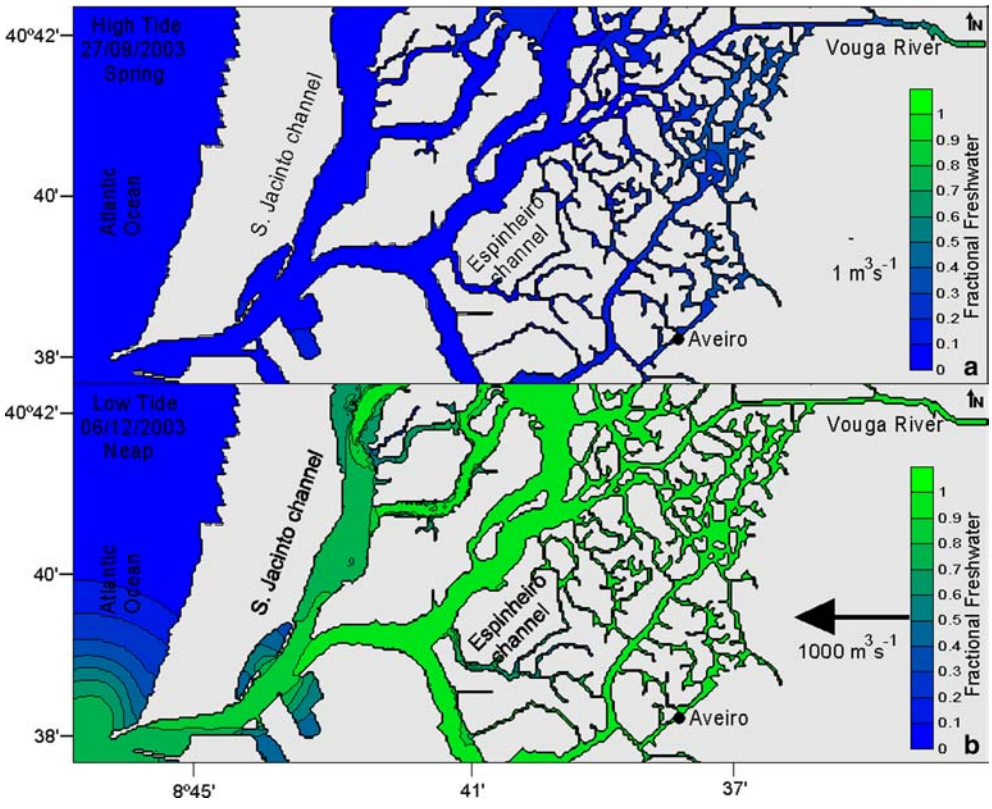

Fig. 11 Fractional freshwater concentrations. **a** minimum quantity of water within the channel (high tide, spring tide period of 26/09/2003) and **b** maximum quantity of water within the channel (low tide, neap-tide period of 06/12/2003).

field data. When the river flow is weak, the saline and thermal fronts are well reproduced by the model as previously showed. When the river flow is high, even thought the model results are consistent with the expected patterns, it would be more adequate to study the transport processes using the model in a 3D mode, in order to reproduce the vertical stratification found from the measurements. Due to the complexity of the study area, this is a very difficult task, which is presently being performed. It can be considered that Mohid was successfully implemented and that it is a useful tool to study transport processes in complex estuarine environment.

Results obtained with a Lagrangian approach by Dias et al. (2003) are in agreement with the present conclusions confirming the importance of these channels from the hydrodynamic and transport perspective. Trajectories of passive tracers released along the channel revealed that the transport was towards the lagoon's mouth. These results indicate the low residence time of the central area of the lagoon and the importance of the water exchanged between the channel and the ocean.

In the future results from the 3D model will be studied in order to perform better hydrodynamic and transport studies in this area.

Acknowledgements The first author of this work has been supported by the University of Aveiro through a PhD grant and by the FACC fund of the Portuguese FCT.

References

Abbot MB, Damsgaardand A, Rodenhuis GS (1973) System S21, Jupiter, a design system for two-dimensional nearly-horizontal flows. J Hyd Res 1:1–28

Arakawa A, Lamb V (1977) Computational design of the basic dynamical processes of the UCLA general circulation model. Mon Weather Rev 125:2293–2315

Barnes RSK (1977) The coastline. Wiley, Chichester, UK, p 356

Barnes RSK (1980) Coastal lagoons. Cambridge University press, Cambridge, p 106

Castanho JP, Carvalho R, Vera-Cruz D (1968) Barragem no rio Vouga e desvio dos esgotos–anteprojecto (55 pp), unpublished report, II

Chippada S, Dawson C, Wheeler M (1998) A godonov-type finite volume method for the system of shallow water equations. Comput Methods Appl Mech Eng 151:105–130

Cressie NAC (1993) Statistics for spatial data–revised edition. John Wiley & Sons, New York, p 900

Dias JM (2001) Contribution to the study of the Ria de Aveiro hydrodynamics. PhD Thesis, University of Aveiro, Portugal

Dias JM, Lopes JF, Dekeyser I (1999) Hydrological characterisation of Ria de Aveiro, Portugal, in early summer. Oceanologica Acta 22(5):473–485

Dias JM, Lopes JF, Dekeyser I (2000) Tidal propagation in Ria de Aveiro lagoon, Portugal. Phys Chem Earth (B) 25:369–374

Dias JM, Lopes JF, Dekeyser I (2001) Lagrangian transport of particles in Ria de Aveiro Lagoon, Portugal, Phys Chem Earth (B) 26(9):721–727

Dias JM, Lopes JF, Dekeyser I (2003) A numerical system to study the transport properties in the Ria de Aveiro lagoon. Ocean Dynamics 53:220–231

Dias JM, Fernandes, E.H. (2005) Tidal and subtidal propagation in two Atlantic Estuaries: Patos Lagoon (Brazil) and Ria de Aveiro Lagoon (Portugal). J Coastal Res, SI39 (in press)

Dronkers JJ (1964) Tidal computations in rivers and coastal waters. North-Holland Publishing Company, Amsterdam
Dyer KR (1997) Estuaries: a physical introduction, 2nd edn. John Wiley & Sons, New York, p 195
Ferziger J, Peric M (1995) Computational methods for fluid dynamics. Springer, New York
Kjerfve B (1994) Coastal lagoons processes. In: Kjerfve B (ed) Coastal lagoons processes. Elsevier Oceanography Series, Amsterdam, n°60, pp 1–8
Leendertse J (1967) Aspects of a computational model for long water wave propagation, Memorandum RH-5299-RR. Rand Corporation, Santa Monica
Leendertse J, Liu S (1978) A three-dimensional turbulent energy model for non-homogeneous estuaries and coastal sea systems. In: Nihoul J (ed) Hydrodynamics of estuaries and fjords. Elsevier, Amsterdam, pp 378–405
Lopes JF, Dias JM, Dekeyser I (2001) Influence of tides and river inputs on suspended sediment transport in the Ria de Aveiro lagoon, Portugal, Phys. Chem Earth (B) 26(9):729–734
Martins F, Leitão P, Silva A, Neves R (2001) 3D modelling in the Sado estuary using a new generic vertical discretization approach. Oceanologica Acta 24(1):1–12
Moreira MH, Queiroga H, Machado MM, Cunha MR (1993) Environmental gradients in a southern estuarine system: Ria de Aveiro, Portugal, Implications for soft bottom macrofauna colonization. Neth J Aquat Ecol 27(2–4):465–482
Pawlowicz R, Beardsley B, Lentz S (2002) Classical tidal harmonic analysis including error estimates in MATLAB using T_TIDE. Computers & Geosciences 28:929–937
Vaz N, Dias JM, Leitão P (2004) Hydrodynamical modelling of the Ria de Aveiro lagoon: Mohid's preliminary calibration. Proceedings of Littoral 2004: pp 774–775
Vicente CM (1985) Caracterização hidráulica e aluvionar da Ria de Aveiro, Utilização de modelos hidráulicos no estudo de problemas da Ria, in: Jormadas da Ria de Aveiro, III, Edição da Câmara Municipal de Aveiro, Portugal pp 41–58
Vinokur M (1989) An analysis of finite-difference and finite-volume formulations of conservation laws. J Comput Phys 81:1–52